The mechanism producing initial transients on the clarinet

A. Almeida, W. Li, J. R. Smith, et al.

Citation: The Journal of the Acoustical Society of America **142**, 3376 (2017); doi: 10.1121/1.5014036
View online: https://doi.org/10.1121/1.5014036
View Table of Contents: https://asa.scitation.org/toc/jas/142/6
Published by the Acoustical Society of America

The mechanism producing initial transients on the clarinet

A. Almeida,[a] W. Li, J. R. Smith, and J. Wolfe
The University of New South Wales, Sydney, New South Wales 2052, Australia

(Received 19 May 2017; revised 3 November 2017; accepted 8 November 2017; published online 4 December 2017)

In self-sustained instruments, starting transients are important timbral characteristics that help identify the instrument and the playing style. Often, the oscillation starts as a growing exponential. This study investigates the starting amplitude of this exponential for the clarinet. After a rapid tongue release, the reed quickly returns to its equilibrium position. The sudden change in aperture produces an abrupt change in both the airflow into the mouthpiece and the mouthpiece pressure. This perturbation travels along the bore and reflects at the open end. Returning to the mouthpiece with slight attenuation, the perturbation can be amplified by the reed acting as an active element—effectively a negative resistance. When the reed release time exceeds the time for sound to travel twice the bore length, the airflow and pressure wave into the bore via the aperture are superposed over their own returning reflection. Measurements of reed motion and mouthpiece pressures during reed release yield values that are used in a model to calculate waveforms showing similarities to those observed experimentally. The initial amplitude decreases with increasing reed release time, though not always monotonically. It can become very small in special cases due to synchronisation between the initial pulse and its reflection. https://doi.org/10.1121/1.5014036

[TRM] Pages: 3376–3386

I. INTRODUCTION

Attacks or initial transients are an important part of wind instrument performance and expression (e.g., Brymer, 1977; Thurston, 1977; Gingras, 2004; Sullivan, 2006). Perceptually, they play an important role in the recognition of the timbre of the instrument (Saldanha and Corso, 1964). A number of articulations are used for different musical techniques, and these are executed in different ways by different musicians (Li *et al.*, 2016a). Musicians control several parameters, including the blowing pressure and how it varies with time, the lip force, and the coordination of the tongue release with the blowing pressure.

Acoustically, the clarinet is probably the most studied reed instrument and it is in some ways the simplest. An approximately cylindrical resonator means that its acoustic response can be approximated by a delayed impulse, and the single reed is a simpler valve than the double reed (Almeida *et al.*, 2007). Hence it is a suitable instrument for studying how tonguing produces the initial transient on a wind instrument. Furthermore, the clarinet has been thoroughly studied both in the time-domain (Schumacher, 1981) and in the frequency-domain (Silva *et al.*, 2008). For instance, the quasi-static relation between pressure and flow at the reed (Dalmont *et al.*, 2003) is well known and makes it easy to determine the pressure threshold for playing or the relationships between blowing pressure, lip force, and sound level (Dalmont *et al.*, 2005), playing frequency (Bak and Dolmer, 1987), or spectral content (Kergomard *et al.*, 2000) in the steady-state.

Most studies on clarinet acoustics have concentrated on the sustained part of a note. Recently, the present authors showed that the transient includes a stage during which the oscillation in the resonator grows at an exponential rate and measured how the rate of this growth depends on blowing pressure and lip force (Li *et al.*, 2016b). This paradigm can be extended to situations when the control parameters vary during the transient, producing a note with a varying exponential rate (Bergeot *et al.*, 2014). A sudden change in the rate of increase of the blowing pressure is sometimes expected to cause a discontinuity in the amplitude of the sound (Almeida *et al.*, 2015).

The exponential phase ends as the note approaches saturation, i.e., once the amplitude of the pressure variation in the mouthpiece becomes comparable with the blowing pressure. The value of the amplitude at the start of the exponential phase therefore plays an important role in determining the duration of the transient. Understanding the cause of this initial amplitude and how it depends on the blowing pressure and the initial displacement and motion of the reed is the main aim of this study.

A previous study (Li *et al.*, 2016b) indicated that, after release from the tongue, the reed approaches mechanical equilibrium. The associated change in aperture creates an acoustic perturbation that propagates down the bore, is then reflected and, following successive interactions with the reed, establishes a standing wave. Using a clarinet in its usual configuration, it is difficult to investigate the phenomena involved for three reasons. First, both the bell and the

[a]Electronic mail: a.almeida@unsw.edu.au

open tone hole array have a cutoff frequency and other frequency dependent properties, so the reflected pulse is distorted and may sometimes be hard to identify. Second, the lowest note on the clarinet has a nominal frequency of 147 Hz, so the return of the first reflection occurs after about 3 ms or less. This makes it hard to separate the initial pulse, whose duration may also be several ms or more, from its reflection. Third, the acoustical impedance of the vocal tract or the artificial mouth in a playing machine can complicate the airflow and reed motion.

The first problem can be solved by replacing the clarinet bore with a cylindrical pipe of similar diameter, open at the end remote from the mouthpiece, but without a bell. The second can be solved by making that pipe rather longer than a normal clarinet. Third, the mouth impedance can be reduced to be much smaller than that of the bore. The present study uses a mechanical lip and tongue and a controlled pressure source to "play" a clarinet mouthpiece and reed connected to a long cylindrical pipe. Rather than blowing at the mouthpiece, suction is applied to a reservoir connected to the remote end of the pipe. Thus the air in the laboratory surrounding the mouthpiece, which has a very large compliance, becomes the very small "mouth" impedance.

The experimental apparatus used in this article is described in Sec. II. In the first study presented here, the pipe acting as a resonator is 3 m long. With this apparatus, the mechanical responses of reeds are measured with and without a lip and with and without blowing pressure for a range of different initial reed transients (Sec. III A). These results are used to test a simple model for the initial acoustic wave that is similar to the "water hammer" phenomenon in hydraulics (Sec. III B). The water hammer describes the propagation of a sudden change in pressure produced when the flow in a pipe is rapidly stopped by closing a valve (Chaudhry, 1979; more details below).

In further experiments, shorter cylindrical resonating pipes are used so that the reflected wave can interact with the pressure perturbation produced by the change in reed opening (Sec. III D). These results are compared with calculations using simple models for the initial pressure perturbation and the traveling wave it initiates. Further experiments conducted when the mechanical damping provided by the lips is removed give some insights into the production of "squeaks" (Sec. III E).

II. MATERIALS AND METHODS

A clarinet mouthpiece (Yamaha, Japan; model CL-4C) is connected to completely cylindrical pipes of different lengths, rather than to a normal clarinet bore. The inner diameter of the pipes, 15 mm, is similar to that of the clarinet bore. The apparatus is aspirated rather than blown: the far end of the pipe is terminated with a low-pressure reservoir that is lined with acoustic foam to provide a low impedance reflection condition. The (negative) pressure in the reservoir is maintained by a pump (Positive airways pressure model R261-708, ResMed, Sydney, Australia). The reservoir volume is 63 litres.

The exteriors of the mouthpiece and reed are exposed to atmospheric pressure in the laboratory. This arrangement ensures that the acoustic load on the upstream side of the reed is negligible at all frequencies of interest. Further, it allows easy access to the reed, simpler control of the tonguing mechanism, and optical access to the reed for high-speed video recording. Because the mouth is at atmospheric pressure, the mouthpiece gauge pressure P is negative. The blowing pressure will be referred to as P_{blow}, which is calculated as $-P_0$, the initial value of $-P$. In the remainder of the article, varying physical quantities are represented by capital variables, and can be decomposed into a reference value (with index 0, P_0 for example); usually the value before the reed is released, and the difference relative to this reference, represented by the lower case (for example, p). For the mouthpiece pressure the reference is the measurement before the reed release, $P = P_0 + p = -P_{\mathrm{blow}} + p$, so an increase in p in the mouthpiece pressure makes P less negative.

For ease of use, the reed is facing upwards, which is opposite the usual use in clarinet playing (Fig. 1). A small slab of polyurethane (Sorbothane, Kent, OH) simulating the lip is pressed against the reed by a suspended mass. This provides a constant, known, and adjustable lip force applied to the reed (up to 1.2 N in this study). The slab is 11 mm wide, 13 mm long, and 4 mm thick with the masses hanging at the centre position, located 14 mm from the reed tip.

For most experiments, a synthetic clarinet reed (Légère Reeds, Ontario, Canada, hardness 3) is used. In one initial experiment, a cane reed (Rico, Farmingdale, NY, hardness 3) is also used.

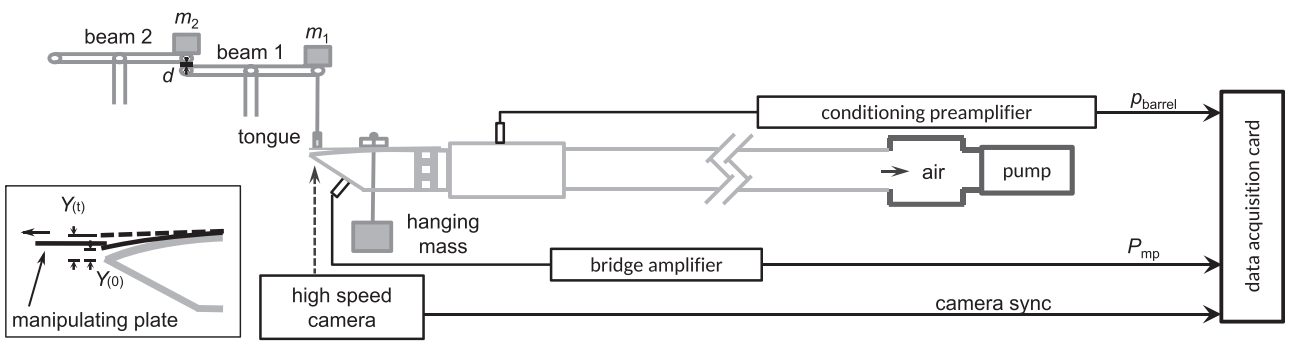

FIG. 1. The experimental setup (not to scale). The controlled acceleration mechanism, with two masses, is shown in the main picture. The manipulating plate setup is shown in an inset.

Notes are initiated in three different ways. In all, the reed is attached to the mouthpiece with a ligature, as usual. In the first (plate-release) method, a thin plate is clamped in a two-dimensional micromanipulator, as shown in Fig. 1. The tip of this manipulating plate is positioned so as to pull the tip of the reed the desired distance up and away from the mouthpiece. The plate is then withdrawn (in a direction parallel to the axis of the clarinet), releasing the reed and allowing its elasticity to bring the reed back to near its equilibrium position. The plate is also used to push the reed down toward the mouthpiece, then suddenly released. Except for a change in sign, the results of the former experiments are very similar and are not reported here. With this method, the motion of the reed after release is determined by reed mechanical properties and cannot be experimentally controlled.

The second method (controlled acceleration) uses a small slab of the same polyurethane to act as an artificial tongue, as shown also in Fig. 1. This tongue pad is operated by two beams mounted on axles. First, the pad is pushed against the reed by a known force (controlled by mass m_1) in the direction that closes the reed onto the mouthpiece. This tongue pad can be accelerated away from the reed at controlled rates of acceleration using the second pivoted beam (with acceleration controlled by mass m_2).

In a third (manual) method, beam 2 in Fig. 1 is removed when investigating large variations in tongue acceleration and the experimenter presses the left end of beam 1 with a finger. It is difficult to produce a specific value of acceleration with this method, but it can produce a larger range of tongue acceleration than the 2-beam system (see Li *et al.*, 2016b, for more details of the second and third methods). From a sufficient number of trials, transients that approximate the desired values may be chosen.

During the experiments, video recordings are made of the motion of the tongue and reed using a high-speed camera, recording 8000 frames per second. The reed displacement $y(t)$ from its initial position is determined from analysis of the frames, and the acceleration is determined by fitting a parabola with zero initial slope to $y(t)$. Simultaneously, the pressure in the mouthpiece, P_{mp}, is measured with a transducer (8507C-2, Endevco, Irvine, CA) inserted in the mouthpiece (30 mm away from the reed) and recorded using a digital acquisition card (NI9234, National Instruments, Austin, TX) at 51 200 samples per second. A microphone and conditioning amplifier (4944A, Brüel & Kjær, Nærum, Denmark) measure the sound pressure at a distance of 95 mm downstream from the reed tip. (This position, corresponding to a location within the barrel of a clarinet, was chosen to reduce the level of turbulence recorded and is hereafter called the barrel pressure p_{barrel}.)

III. RESULTS AND DISCUSSION

A. Generation of a pressure pulse by the reed without a continuous airflow

A reed can vibrate freely as a cantilever beam at its own resonant frequency, determined by its mechanical properties and geometry. Examples of this vibration, triggered by an initial displacement, are shown in Fig. 2.

In this experiment, the tip of the reed is pressed toward the mouthpiece a distance of ~0.25 mm, using the plate-release method described above, and suddenly released. Four different reed conditions are used. Two conditions used a cane reed without a lip, dry in a first trial and for the second trial soaked in water for 30 s and then wiped with a tissue. A synthetic reed (always dry) was used both without and with the pad used as part of an artificial lip, but in both cases without the hanging mass used to apply lip force. The first row of subfigures (plots labeled with "A") shows the reed displacement $y(t)$ from its initial position before release (initial displacement is indicated by zero in Fig. 2 and hereafter); the second (label "B") shows the pressure in the mouthpiece and the third (label "C") the magnitude of that pressure expressed in dB.

Normally the sound generated by a vibrating reed would travel down the bore of the clarinet and return quickly to interact with the reed during the reed's motion. To avoid this complication, the "clarinet" in these experiments was a 3.00 m pipe with a barrel that adds 3 cm, and a mouthpiece that gives a total length of 3.12 m and thus a round trip time of 18 ms. In each of the examples in Fig. 2, the attenuated echoes are observed after 18 and 37 ms.

The dry cane reed (plots A1, B1, and C1) has the highest natural frequency. (Cane reeds are usually not played dry: players usually wet them before playing, and they are kept moist by the player's breath.) The synthetic reed with an attached lip pad exhibited the lowest natural frequency because of the extra mass. Without that pad, the natural frequencies range from 1280 to 1400 Hz, which is toward the top of the normal playing range of the clarinet (say, sounding *F*6 on a Bb clarinet or nominally 1400 Hz). From the exponential decays of the oscillation $y(t)$ in Fig. 2, Q factors are calculated: 17.0 ± 0.9 (dry cane, column 1), 19.5 ± 3.4 (wet cane, column 2), 7.4 ± 1.1 (synthetic, column 3), and 5.1 ± 0.5 (synthetic with lip, column 4). The damping in these conditions is lower than in normal playing because the lip pad moves with the reed as a compact mass and provides relatively little mechanical damping. Since the behaviours of the different reeds shown in Fig. 2 are qualitatively similar, only the synthetic reed is used in the subsequent experiments. Synthetic reeds have the advantage that they can easily be played dry and have stable physical properties during long studies (Almeida *et al.*, 2013).

When a lip force is provided by a hanging mass (tens of grams in this study), the lip pad is subjected to a force from the vibrating reed and a tension resulting from the weight and inertia of the mass. Under these conditions, the motion of the reed is more strongly damped (Fig. 3). In normal playing, the player's bottom lip would be subjected to a vibrating reed on one side and forces related to the inertia of the jaw on the other. This condition should also damp the reed motion.

B. The initial impulse produced by the change in reed opening

Figure 3 shows example results of experiments in which the transient is initiated using different controlled upwards

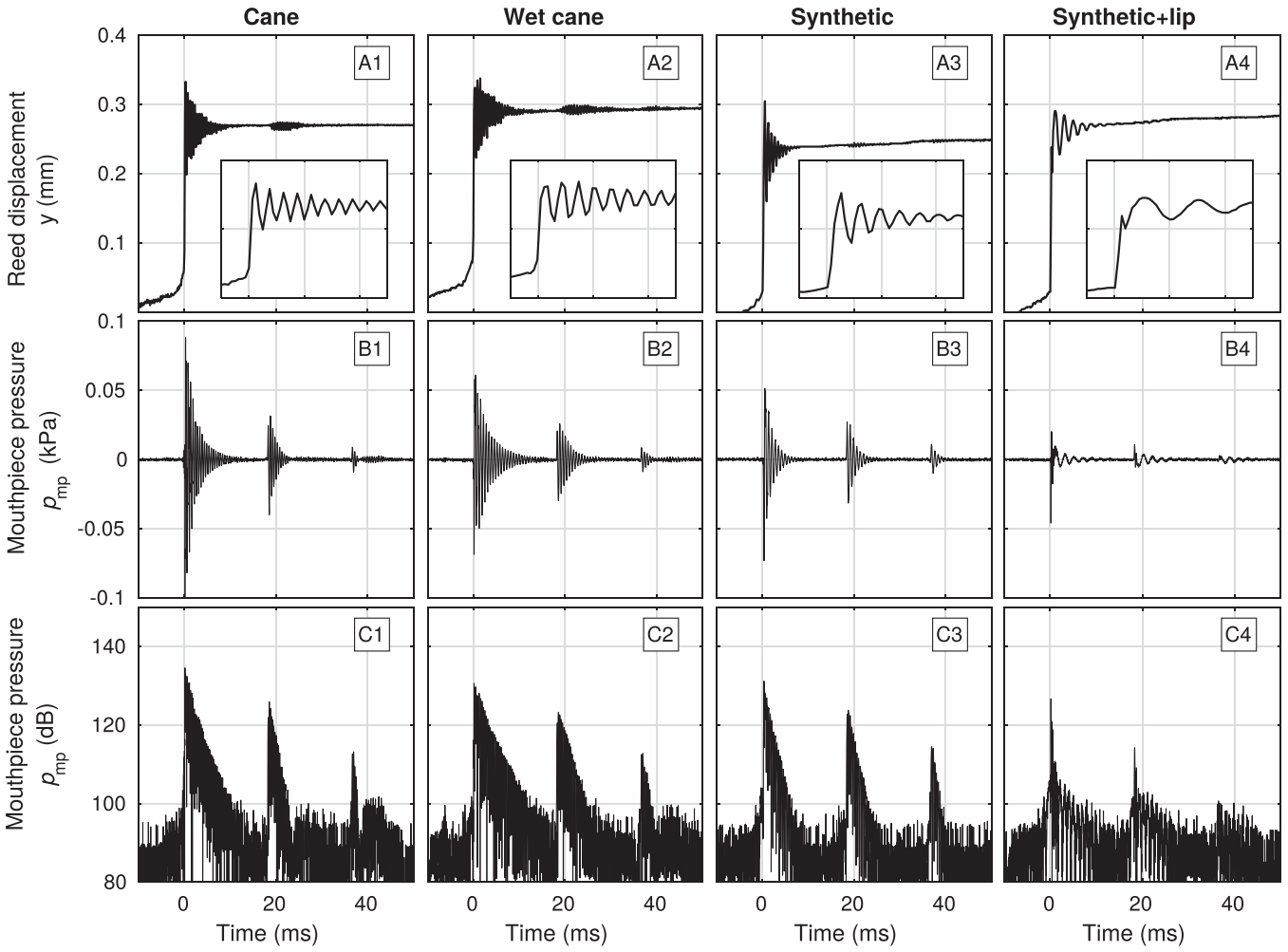

FIG. 2. Oscillation of the reed when suddenly released, with no blowing pressure. The top figures show the tip displacement $y(t)$ from its initial position, measured from the camera images. The pressure pulse initially generated by the reed oscillation is reflected at the open end of the pipe and returns to the mouthpiece after 18 ms. In each case, the inset shows the beginning of the transient with an expanded time scale spanning 6 ms and a vertical scale spanning 0.4 mm. The acoustic pressure in the mouthpiece is shown on a linear scale in the second row and its magnitude is shown in a logarithmic scale $20\log_{10}(|p_{mp}|/20\,\mu\text{Pa})$ in the third row.

accelerations of the synthetic reed. The lip force was 0.7 N in each case. These experiments use a 0.89 m pipe connected to the mouthpiece and barrel instead of a clarinet (with a round-trip time lasting 5.8 ms as indicated by the horizontal bar). The top row of the plots [Figs. 3(a) and 3(b)] shows the displacement y of the reed tip from its initial position, and the lower shows the acoustic pressure p_{barrel} in the barrel position rather than in the mouthpiece, which has more turbulent noise. This introduces a delay of 0.3 ms between measurements in the barrel with respect to the mouthpiece. In these experiments, the blowing pressure (the average pressure difference across the reed) was 5.5 kPa.

In this experiment, moving the reed away from the mouthpiece shows a new effect; air enters the mouthpiece through the enlarged aperture and the mouthpiece pressure increases by about 0.2 kPa over about 2 ms. Note that this initial variation in pressure is approximately proportional to the reed displacement, and thus to the area of the aperture between reed and mouthpiece. After the initial change in y, there are some small amplitude, high frequency oscillations in y near the reed's new equilibrium position, and similar oscillations are also seen in the barrel acoustic pressure, p_{barrel}. These oscillations are much smaller than those in Fig. 2 because, as explained above, applying the lip force damps oscillations at the reed's natural frequency.

After about 6 ms, the pressure perturbation returns inverted after acoustic reflection at the remote end of the pipe. If the pipe were ideally open at the remote end (reflection coefficient -1) and ideally closed at the reed (reflection coefficient 1), then the amplitudes of the positive and negative excursions would be equal, in the absence of losses. In that case (ideal reflections, no losses), the first negative pulse in $p_{\text{mp}}(t)$ (near 8 ms) would have twice the magnitude of the initial rise (near 2 ms), because of superposition of the reflection on the signal. In practice, the magnitude of the factor is greater than 2, because of the amplification by the reed.

The variation in $y(t)$ around 8 ms shows that the reed is not a rigid reflector: it is displaced by the returning acoustic pulse. Further, its displacement changes the aperture and thus the airflow and pressure. Note that, here, the arriving

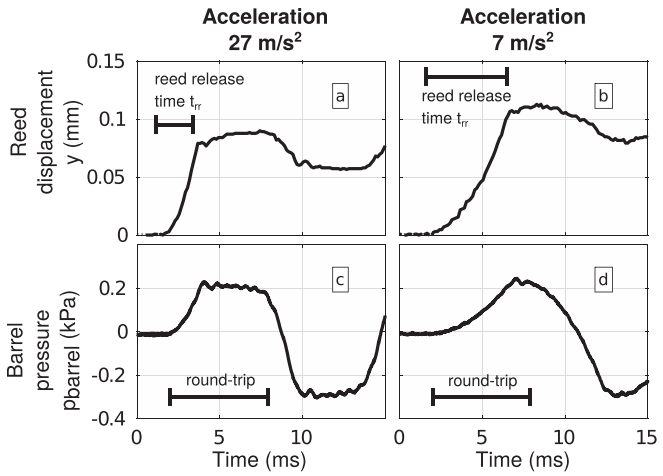

FIG. 3. The reed displacement y (measured from its initial position) and barrel acoustic pressure p_{barrel} during and immediately after the "tongue" releases the synthetic reed from a position where it is pressed toward the mouthpiece by a tongue force 0.2 N. The lip force was 0.7 N and blowing pressure 5.5 kPa. The pipe is 0.89 m long which, with barrel and mouthpiece, gives a round trip time of 5.8 ms, as shown by the horizontal bar. The pressure change has a shape similar to that of the reed displacement until the reflected acoustic wave comes back from the opposite end of the pipe. Notice that when the tongue release is slower (right) the pressure rise is also slower.

negative pressure pulse acts to close the reed and thus to amplify the negative pulse. Similarly, the returning positive pulse at 15 ms tends to open the reed, admitting more flow and increasing the pressure. These amplification effects on the subsequent evolution of the standing wave will be discussed quantitatively later.

1. The initial perturbation: The water hammer model

Figure 4 illustrates a variant on the water hammer effect, with the difference that the sketch shows a sudden increase in airflow, while the water hammer in plumbing is usually produced by a reduction in water flow caused by closing a tap. In the sketch, a suddenly increased aperture has admitted air at slightly higher absolute pressure and density, with the interface between high and low pressure regions propagating at the speed of sound c.

In the present experimental system, the mouth is at atmospheric pressure P_A (Fig. 4). The remote end of the pipe is at (negative) gauge pressure P_0 (so the blowing pressure is $P_{\text{blow}} = -P_0$ and the initial mouthpiece pressure is P_0). The aperture through which air flows past the reed is $S = wY$, where Y is the vertical distance between the reed tip and the mouthpiece and w is the effective width of the aperture.

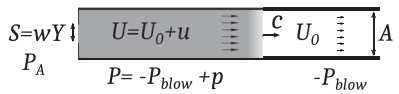

FIG. 4. Schematics comparing the current experiment with the water-hammer: The air is initially flowing through an opening $\boldsymbol{S_0}$ at a rate $\boldsymbol{U_0}$ into a pipe, which is initially at gauge pressure $-\boldsymbol{P_{\text{blow}}}$. The opening (here equal to $\boldsymbol{wY}$) then increases to $\boldsymbol{S}$ producing a region with flow $\boldsymbol{U}$ and gauge pressure $\boldsymbol{P} = \boldsymbol{P_{\text{blow}}} + \boldsymbol{p}$, where $\boldsymbol{p} \ll |\boldsymbol{P_{\text{blow}}}| \ll \boldsymbol{P_A}$. The boundary region with increased pressure travels downstream at speed $\boldsymbol{c}$, as shown.

Assuming that the kinetic energy gained by the air flowing through the aperture is lost in turbulence in the mouthpiece, the volume flow and blowing pressure are related by the "Bernoulli term,"

$$U = S\sqrt{\frac{-2P}{\rho}}, \tag{1}$$

where ρ is the density of the air. Throughout this calculation $p \ll |P_0| \ll P_A$. ρ can vary slightly because of the variation in pressure. However, the change in density is of second order since ρ/ρ_0 is on the order of p/P_A. The value of ρ_0 will be used in the following.

Consider a hypothetical case where, at time $t = 0$, there is a discontinuous reed displacement y, leading to an immediate increase in the flow into the mouthpiece.

This step change in flow produces a column of air with slightly higher pressure and density. The air in that column is traveling down the pipe with speed $(U_0 + u)/A$, which is greater than the flow on the downstream side of the pressure discontinuity (U_0/A).

The length of this column is ct, the distance that the pressure discontinuity travels at the speed of sound c into the pipe (the bore in the case of a clarinet). For a pipe of cross section A, the extra mass of this column is $\rho_0 Act$, so the extra momentum of this column due to its extra speed is $mv = (\rho_0 Act)(u/A)$. From Newton's law, the time derivative of this momentum gives the force due to the discontinuity in pressure acting at the position of the density discontinuity: $pA = \rho_0 cu$, so

$$p = \rho_0 c\frac{u}{A}, \tag{2}$$

which has similarities with the water hammer effect (Chaudhry, 1979). Equation (2) can also be derived directly by considering the characteristic impedance of the pipe $Z_c = \rho_0 c/A$. Introducing a step increase of flow u produces (before any reflections) a pressure increase of $Z_c u$.

Relating this to the reed position Y, and substituting for u,

$$p = \rho_0 c\, w\frac{y}{A}\sqrt{\frac{2P_{\text{blow}}}{\rho_0}}. \tag{3}$$

Considering a series of small pressure changes over time, the pressure variation is given by

$$p(t) = \left(\frac{wc}{A}\sqrt{2\rho_0 P_{\text{blow}}}\right)y(t). \tag{4}$$

In the experimental sections of this study, $y(t)$ is measured using high speed video and the blowing pressure P_{blow} and the downstream pressure variation $p(t)$ are measured by a pressure transducer in the mouthpiece or barrel. All the other quantities are known or measured, so the applicability of this model can be tested by comparing $p(t)$ and $y(t)$, the change in reed tip position, or by using $y(t)$ to calculate $p(t)$ and then comparing calculated and measured $p(t)$.

2. Experimental comparison with the water-hammer model

In Fig. 3, the similarity in shapes between $p(t)$ and $y(t)$ provides some evidence for an instantaneous proportionality between the reed displacement y and the ensuing pressure perturbation p in the resonator. More evidence comes from comparing the total pressure jump with the total reed displacement, measured between the instant the reed starts moving and when it comes to mechanical equilibrium [e.g., from zero to about 3 and 7 ms in Figs. 3(a) and 3(b), respectively]. In the simple model, the ratio of these two changes is the proportionality coefficient $((wc/A)\sqrt{2\rho_0 P_{\text{blow}}})$ as given by Eq. (4).

Figure 5 shows the pressure change calculated from Eq. (4) plotted against the measured pressure change. The parameters A, P_{blow}, and ρ_0 are known and the geometrical width of the mouthpiece slot (11 mm) is used for w. The model, which has no adjustable parameters, fits approximately, but does not show the slightly stronger than proportional dependence of p on y suggested by Fig. 5. Error bars are the result of noise in the measured $y(t)$ due to the limited spatial resolution of the camera. The calculation could be in error for two reasons. First, air may enter past the sides of the reed as well at the end, which would increase the effective width. On the other hand, because streamlines have to bend around sharp corners of the inlet (in particular the reed edge), the effect of the *vena contracta* (Hirschberg, 1995) is to reduce the equivalent cross-section of the channel and thus w in Eq. (4).

C. Acoustic oscillation and regeneration

When a lip force is applied, the reed is damped and this, combined with its stiffness, means that the immediate acoustic effect of the initial reed motion—arising from the proportionality of $p(t)$ and $y(t)$ due to the varying flow—is of short duration. Further, once the reflection of the pressure pulse returns, $p(t)$ begins to influence $y(t)$, as well as the reverse. In Fig. 6, the top row shows the initial several cycles of the oscillation of a synthetic reed with the 3 m long pipe at three different values of the blowing pressure. The transient is initiated with the controlled acceleration system. The gray lines in the second row are the change in pressure p_{mp} measured by a pressure transducer located in the mouthpiece, 30 mm away from the reed tip. This signal includes the continuous pressure offset, but is noisy because of the turbulence of the high-speed flow in this area. The black lines in the second row are the acoustic pressure p_{barrel} measured in the bore by a microphone 95 mm downstream. Here, where the air speed is much slower, the turbulent noise is less and the signal is filtered by the microphone high-pass response at 8 Hz. As in Fig. 2, the inset shows a 6 ms sample of the main curve, including the beginning of the transient. The last row shows the logarithm of the absolute value of the pressure.

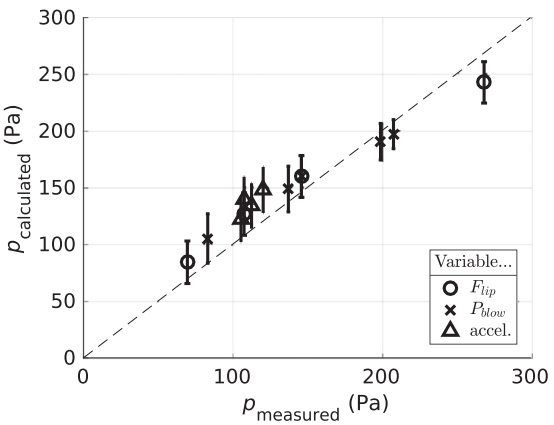

FIG. 5. The relationship between the measured pressure perturbation p and that calculated from the measured change in reed aperture. Data points are from experiments where the lip force ($\boldsymbol{F}_{\text{lip}}$), the blowing pressure ($\boldsymbol{P}_{\text{blow}}$), or reed acceleration were varied. Vertical bars show the estimated uncertainty in calculated pressure mainly due to the pixel resolution in the measurement of reed displacement.

The first column of plots (A1, B1, and C1) shows a typical result with a blowing pressure of zero, reproducing one of the cases in Fig. 2. The small mechanical oscillations of the reed are visible in the zoom insets. The small (noisy) pressure variations visible on the log plot are again spaced by the 18 ms round trip imposed by the 3 m pipe. When the blowing pressure is below the threshold for auto-oscillation (A2, B2, and C2), the water-hammer pressure jump is visible at $t = 0$. As in Fig. 3, the pressure jump returns inverted, with slightly smaller amplitude. Here it is reflected at the reed end, which is, to a crude approximation, a closed termination. After two round trips (36 ms), the cycle is repeated, each time with reduced amplitude. (In the second and third columns, the slow rise in mouthpiece pressure is partly due to the finite compliance at the downstream end of the pipe, which lowers gradually the blowing pressure, and partly due to the mechanical relaxation of the reed.)

In the third column (A3, B3, and C3), the blowing pressure is above threshold, so each reflected water-hammer step produces a pulse whose amplitude increases in successive cycles. The shape of the waveform shows that, while the fundamental (H1) is increasing in amplitude, the highest harmonics (H3, H5) responsible for the sharp corners in the waveform are attenuated over the time scale shown here. In the logarithmic plot of the acoustic pressure amplitude, an exponential rise is observed. The exponential rise rate (and thus the gain coefficient) is 48 dB s^{-1}. The middle column (A2, B2, and C2) shows a decrease that is approximately exponential: below the threshold, the regenerative energy produced by the reed is less than that lost in the pipe and by radiation (exponential rise and decay rates were modelled by Li *et al.*, 2016b).

In these examples, the long pipe (3 m) and the rapid initial motion of the reed together mean that the transient due to the reed's mechanical oscillation can be clearly distinguished from the acoustic reflection. This would not be the case for the clarinet under normal playing conditions, especially for high notes, so Sec. III D reports experiments with a shorter pipe.

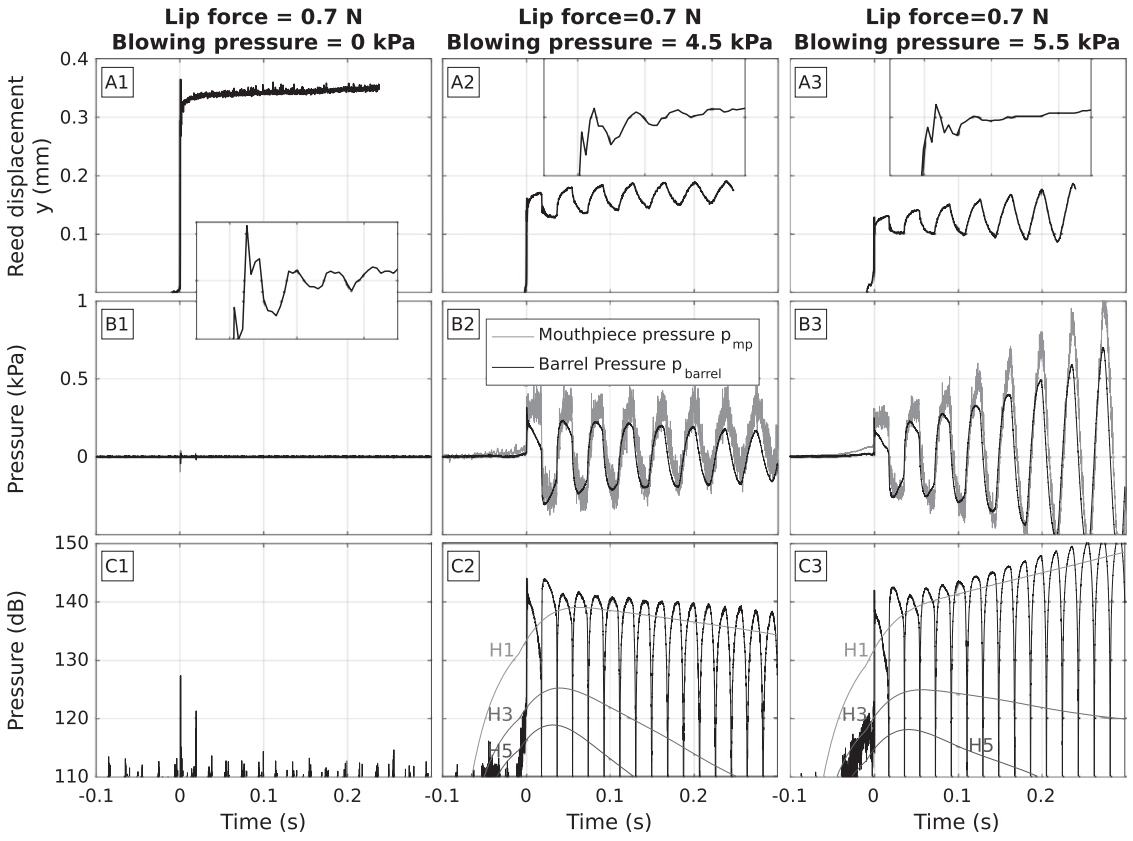

FIG. 6. The initial cycles of the oscillation of a synthetic reed measured with three different values of the blowing pressure P_{blow} but with same lip force of 0.7 N. As in Fig. 2, each inset on plots A1, A2, and A3 shows an expanded (6 ms × 0.1 mm) sample of the reed displacement curve that includes the beginning of the transient around $t = 0$. B1, B2, and B3 show, in gray, the mouthpiece pressure measured by a transducer near the reed. The black curve shows the acoustic pressure in the barrel, measured by a microphone 95 mm downstream from the reed away from the turbulence and high-pass filtered by the microphone (3 dB point at 8 Hz). C1, C2, and C3 show the magnitude of the acoustic barrel pressure on a log scale $20\log_{10}(|p_{\text{barrel}}|/20\,\mu\text{Pa})$, and also the amplitudes of the fundamental, third and fifth harmonics (H1, H3, H5) as extracted by a heterodyne detection algorithm with a window of 150 ms. The pipe is 3 m long, giving a round-trip time of 18 ms. (The threshold for oscillation lies between 4.5 and 5.5 kPa.)

D. Interaction of the reed's mechanical perturbation with the reflected wave

Figure 7 shows transients produced with a 0.89 m pipe connected to the barrel and mouthpiece (giving a total length of 1.01 m, which is about 50% longer than a Bb clarinet). The transient is initiated by the controlled acceleration method for faster initial reed motion, and manual control for slower ones. This allows observation of different extents of superposition of the pressure waves due to the reed's mechanical oscillation and the acoustic waves due to reflections at the end of the pipe. The blowing pressure is set to the same value across all experiments. However, because of the different tonguing conditions, its value changes transitorily following the removal of the tongue (by about 150 Pa or 3.6% of the blowing pressure). This produces different values of the exponential growth constant, which has values in the range 145 ± 14 dB s^{-1}. The lip force is constant for all examples.

The first two cases shown in Figs. 7(a) and 7(b) (accelerations 23.5 and 14.7 m s^{-2}) are the barrel pressure data whose first several milliseconds were plotted in Fig. 3. Here the black lines show the growth of the oscillation as the amplification by the reed continues. The accelerations in Figs. 7(c) and 7(d) (3.2 and 0.9 m s^{-2}, respectively) produced longer durations of the initial mechanical perturbation,

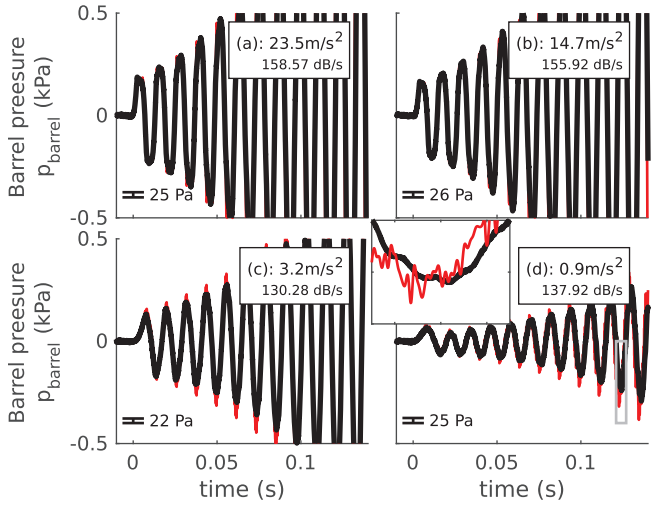

FIG. 7. (Color online) The measured (thick dark line) and predicted (thin pale line) barrel pressure measured in a pipe of 1.01 m total length. The predicted oscillation was calculated from $\boldsymbol{y}(t)$ (see text). The vertical bar shows the expected uncertainty in the calculated pressure due to the camera resolution in y, which is used to calculate the pressure. The inset view of the minimum at 0.13 s shows that the calculation and measurement differ in their high frequency components, in part because of the filtering of the acoustic signal by viscous losses and radiation at the open end of the tube; these losses were not included in the calculation.

so that the initial reed displacement due to tonguing is not yet finished when the first reflected acoustic wave arrives back at the reed. This results in a smaller initial amplitude.

In Fig. 7, the initial displacement of the reed $y(t)$ is used to calculate a pressure perturbation $p_{\text{primary}}(t)$ according to Eq. (4). The thin pale lines [$p_{\text{predicted}}(t)$] are calculated using a mathematical series based on this perturbation

$$p_{\text{predicted}}(t) = \sum_{k=0}^{+\infty} (-G)^k \, p_{\text{primary}}\left(t - \frac{kT}{2}\right). \tag{5}$$

In Eq. (5), G is a gain factor determined from the measured pressure signal (close to 1.1) and $T/2$ is the round trip time (5.94 ms) giving the delay between successive reflections at the reed.

With the exception of some wave shape differences in Figs. 7(c) and 7(d), the agreement is reasonably good. The differences are in part attributable to the noise in $y(t)$ due to the small reed displacements, limited spatial resolution of the camera, viscous losses, radiation losses, and the fact that the calculation does not include the mass of the reed, and so should be inaccurate for the higher harmonics.

1. Simplified tonguing model

Figure 7 and other similar data sets (not shown) demonstrate how the tongue motion, the reed motion, the water-hammer model, and a very simple model for the acoustic response of the pipe are able to reproduce semi-quantitatively two of the main features of the initial transient: the starting amplitude and the consequent waveform. Thus it is possible to obtain a good approximation to the profile of the start of the oscillation simply by superposing the perturbations calculated using the water-hammer model. The remaining differences in shape between calculation and measurement are chiefly in the high harmonics, and may be due to the neglect of the mass of the reed in the calculation. This gives some confidence that simulation using the water hammer model and superposition of reflections will give reasonable approximations in calculations of how the oscillation grows for different profile shapes and rates of reed opening.

Figure 8 shows simulations of the transients resulting from different reed accelerations. The model for the pipe is deliberately simplistic, including only the delay and a constant amplification with value of 1.05 that mimics the active role of the reed and leaves aside any frequency-dependent losses. The panel at left displays the reed displacement and mouthpiece pressure perturbation, which are proportional before the first reflection. The panel at right displays the pressure signal resulting from the superposition of successive inverted and amplified reflections.

In each calculation, the reed-mouthpiece aperture increases toward the same constant final value, but with different values of the (constant) acceleration of the reed (rather like the experiments illustrated in Fig. 3), resulting in different reed release times t_{rr}. Different values of acceleration produce different waveforms and, especially for slow acceleration, different amplitudes. The change in amplitude is

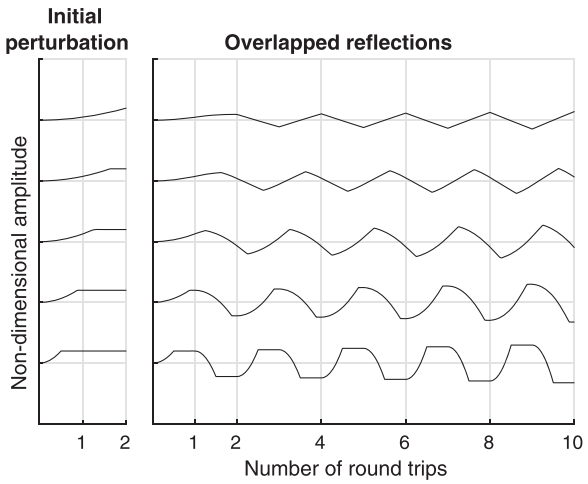

FIG. 8. The left panel shows five different $y(t)$ with the same final amplitude, but different values of accelerations and therefore producing initial pressure perturbations of different durations. Sufficiently large durations of the perturbation (top three cases) will produce smaller amplitudes at the time of return of the first reflection after one round trip. In the right panel, each of these initial perturbations is superposed with successive inverted and amplified reflections. Note that different amplitudes and waveforms result.

largely a consequence of the different degrees of overlap between the opening and the return of the reflected wave. The resulting oscillation has an exponentially growing envelope, due to amplification associated with the active reflection by the reed, here modelled by an imposed amplification coefficient that is similar to that observed in smooth note attacks. Figure 8 shows a relatively short time interval in order to show the details of the waveforms, so the exponential nature of the increase is not obvious in that figure. In these examples, the amplitude of the exponential envelopes decreases as the reed acceleration is reduced, because small accelerations produce only a small reed displacement when the reflected wave first returns. Hence the "clipped" waveform with flattened peaks, like those in Figs. 6(b) and 6(c) and Figs. 7(a) and 7(b), is only produced with the two largest accelerations, for which the reed aperture change is finished before the return of the reflected wave.

It is possible to run these simulations systematically for a range of values of reed acceleration, each having a different reed release time, t_{rr}, and thus yielding different starting values of the exponential growth of the acoustic wave. To calculate this dependence, the exponential envelope of the amplitude of the first harmonic is extrapolated to the moment of tongue release to obtain what is called hereafter the initial amplitude. This initial amplitude is plotted as a function of the reed release time by the black lines in Fig. 9.

The final amplitude at saturation (not shown in Fig. 8) can be approximately calculated from the blowing pressure. The rate of exponential growth is known from the model presented by Li *et al.* (2016b). The duration of the transient can therefore be estimated from the initial amplitude with reasonable precision because the transition from exponential phase to saturation lasts only several cycles (Li *et al.*, 2016a,b). Of course, the high initial amplitudes correspond to short attack transients, because saturation is approached after fewer reed oscillations.

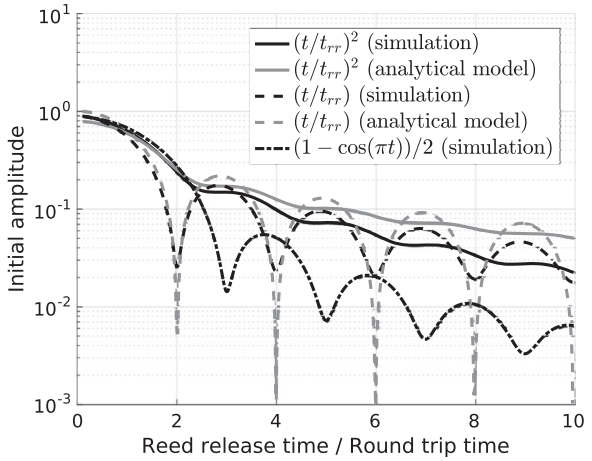

FIG. 9. Semi-logarithmic plot showing how the normalised reed release time affects the calculated dependence of the initial amplitude of the first harmonic. The three curves in black were calculated numerically using different functions for $\boldsymbol{y}(\boldsymbol{t})$. $\boldsymbol{y} = \boldsymbol{f}(\boldsymbol{t})$, $\boldsymbol{0} < \boldsymbol{t} < \boldsymbol{t_{rr}}$, where t_{rr} is the reed release time in the absence of a returning reflection. The time for a round trip is a half period of the note. The initial displacement amplitude is the extrapolation of the exponential envelope of the first harmonic to $t = 0$. The curves in gray were calculated using an approximation to the measured reed motion profiles (details in the Appendix).

In order to calculate the transient duration for a given set of parameters, it is desirable to have an analytical method to calculate the initial amplitude. An approximate method for doing this is presented in the Appendix. Two sets of data calculated using this approximate method are included in Fig. 9 (gray lines) for comparison with the explicit simulations.

In Fig. 9, the overall behaviour is that the initial amplitude decreases as the reed release time t_{rr} increases (tongue acceleration decreases), as also seen in Fig. 8. However, local minima are expected in some of the cases where the reflections of the perturbation profile interfere destructively. These minima are absent for the parabolic $y(t)$, but they appear for linear and sinusoidal $y(t)$ (dashed lines in Fig. 9), i.e., they appear in cases for which the derivatives $y'(t)$ and $y'(t + T/2)$ are similar.

These simulations are consistent with the expectation that a rapid note attack results from a quick release of the reed. They also suggest that, for some reed opening time-profiles, slow attacks may be prone to uncertainty because it may be difficult to match precisely the release time to one of the local maxima or minima shown in Fig. 9. This picture may change for real profiles, which probably do not correspond exactly to any of these functions. Different smooth profiles tend (like the parabolic profile) to have less pronounced maxima and minima. Furthermore, when the reed is released slowly, turbulence and other sources of noise will reduce the effect of destructive interference, smoothing out the minima in the figure.

On a normal clarinet, the longest round-trip time (one-half cycle of the note) is about 3 ms for the lowest note and much smaller for many higher notes. Hence, even if the reed were released by a player as quickly as the plate release method used here, superposition of pulse and reflection would be expected for some notes. It is possible, however, that rather than releasing with the reed with a vertical displacement, the tongue may uncover the reed opening with a movement that is closer to longitudinal. In such a case, the water-hammer effect would be rather more complicated to model.

E. Reed mechanical oscillations and squeaks

In previous results (Secs. III B, III C, and III D), the application of the lip force via the deformable lip pad acts to damp the reed, with the effect that a large fraction of the reed's mechanical energy is lost quickly, rather than establishing an oscillation at the natural frequency of the reed. This is also likely to be the case in normal clarinet playing, when the force from the lower jaw is transmitted to the reed via the soft lower lip. With reduced damping, however, the reed's mechanical oscillations may interact with the returning reflected wave. Depending on the phase between the reed oscillation and the acoustic reflections, oscillation at the reed frequency may sometimes benefit from the gain at the reed, generating a high-pitched sound (Fig. 10), somewhat like the squeak feared by clarinettists.

Figure 10 shows the reed displacement and barrel pressure for transients produced by the manipulating plate release method, with a 3 m long pipe and a blowing pressure of 5 kPa. At left, the reed oscillates freely without the damping of a lip, showing the oscillation at a high frequency determined by the reed, together with that at a low frequency determined by the pipe resonance. At right, with the deformable lip pad and a lip force of 0.7 N, the oscillation at the high frequency is substantially damped. In the case shown in the left of Fig. 10, the oscillations continue to grow quickly to a continuous, saturated, high frequency oscillation (data not shown).

IV. CONCLUSIONS

Controlled initial reed displacements over a range of accelerations show that the initial pressure pulse produced

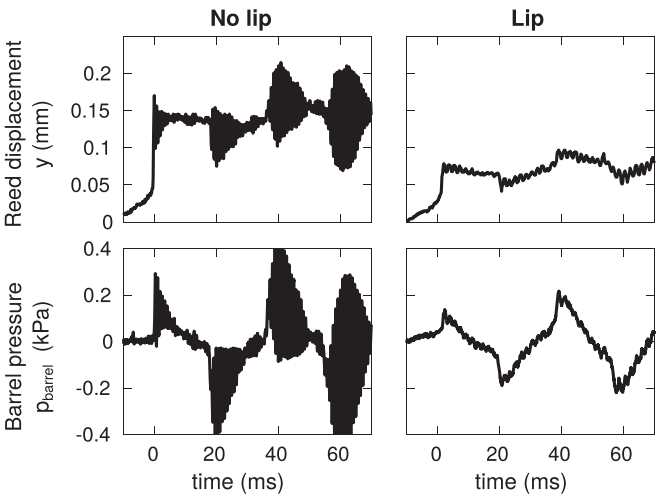

FIG. 10. Initial reed and pressure oscillations when the reed is lightly damped. In both cases, and as in Fig. 2, decaying oscillations at the natural frequency of the reed (about 1300 Hz without lip and 600 Hz with lip) are observed after tongue release at $t = 0$. In the no-lip condition, their amplitude is still visible at the first return of a reflected signal, at about 18 ms. At this moment, the large, inverted pulse is superposed and amplified by the reed. This gives rise to a new, larger pulse of decaying oscillations. Further cycles continue to increase in amplitude. When the lip is applied (with a force of 0.7 N), oscillations at the reed frequency are much more strongly attenuated.

by a moving reed and a blowing overpressure are well approximated to first order by a simple model related to the water hammer effect. As shown in a previous work, the starting transient then follows an exponential envelope, in which the time constant is determined by mouth pressure and lip force. The value of the envelope at the start of the exponential depends on the blowing pressure and how the reed is tongued. When the reed's initial motion is sufficiently fast compared to the travel time of the acoustic wave, the initial amplitude of oscillation is proportional to the change in reed opening during tonguing. When the reed has not reached mechanical equilibrium before the reflected pulse returns (i.e., for high notes or for slow initial reed motion), the two effects are superposed. In these cases, a simple model can reproduce semi-quantitatively some of the main features of the initial amplitude of the acoustic pressure in the bore and the consequent waveform. Simulation results are consistent with the experimental observation: The initial amplitude roughly decreases as the duration of tongue release increases, but may exhibit local minima due to synchronisation between tongue motion and acoustic reflection.

With the models shown here and in previous articles, the duration of the transient thus can be determined from the initial amplitude, the predictable amplitude of the acoustic pressure in the bore at saturation, and the rate of exponential growth.

Under the conditions studied here, the natural frequencies of cane and synthetic reeds without a lip range from 1280 to 1400 Hz and the Q factors range from $\sim$7 to 19. These reeds present qualitatively similar behaviour.

Without damping by the lip, the reed oscillates at its own frequency after tongue release, and this oscillation may be amplified by superposition of reflections from the bore if they are in suitable phase; this behaviour resembles clarinet squeaks.

ACKNOWLEDGMENTS

We thank the Australian Research Council for support of this project, Yamaha for the instrument, Légère for the reeds, and Joe Tscherry and the School of Mechanical and Manufacturing Engineering of UNSW for lending the high-speed camera.

APPENDIX

1. Obtaining starting oscillation amplitudes from *y(t)*

This appendix presents an analytical model to estimate the starting amplitude of an oscillation, given the gain of the reflections and the profile of an initial perturbation that may, in general, overlap the reflections. The first part of the model follows Chap. 4.3 in Chaigne and Kergomard (2016). Because saturation at the end of the transient is rapid, knowledge of the initial amplitude and the gain are sufficient to give a good estimate of the transient duration, hence the interest of an analytical estimation of the initial amplitude.

The method is to treat the exponentially growing transient as a periodic function (the case that would occur with a gain of one) multiplied by an exponential and to obtain the harmonics of one cycle of that transient waveform. For simplification, the case treated has growth factor 1, and oscillations extend from $-\infty$ to $+\infty$. This simplification allows easier calculation of Fourier transforms and alters the shape of the Fourier peaks. The results in terms of the beginning of the oscillation are comparable with simulated ones (as shown in Fig. 9).

2. Initial perturbation

This is defined by a function of time $p_{\text{primary}}(t)$ that is constant for all times except for an interval $[0, t_{rr}]$, where t_{rr} is the reed release time. $p(t) = 0$ for $t < 0$ and $p_{\text{primary}}(t) = p_{\text{primary}}(t_{rr})$ for $t > t_{rr}$.

3. Reflection pattern

A traveling wave $p(x,t)$ travels back and forth in a waveguide, originating from a perturbation $p_{\text{primary}}(t)$ at one end of the waveguide ($x = 0$). In the context of this article, $p_{\text{primary}}(t)$ represents the perturbation caused by the displacement of the reed. The waveform $p(t)$ resulting from successive reflections in the pipe can be calculated using Eq. (5).

Considering the special case where the gain $G = 1$, the oscillation can be extended to negative time without change in the domain under study ($t > 0$), by replacing the lower limit in the sum of Eq. (A1) by $-\infty$. The oscillating function $p(t)$ can be analysed in terms of its Fourier components. In this case, the frequency dependence of the amplitude of p is

$$p'(f) = p_{\text{primary}}(f)\left(\sum_{k=-\infty}^{+\infty} e^{-i2\pi kTf} - e^{-i2\pi(k+1/2)Tf}\right). \tag{A1}$$

This is equivalent to the last equation in Sec. 4.3.2 of Chaigne and Kergomard (2016).

4. Amplitude of individual harmonics

The individual terms of the sum in the previous formula are the amplitudes of each harmonic, if integrated over a narrow interval around each Dirac peak. The amplitude of the kth harmonic is

$$p_k = p_{\text{primary}}\left(\frac{k}{T}\right)\frac{1}{T}\left(1 - e^{-i\pi Tf}\right) \tag{A2}$$

(remembering that p_{primary} is a spectral density and so has units of pressure multiplied by time).

E. Example: Unit ramp

The unit ramp is given as an example,

$$p_{\text{primary}}(t) = \begin{cases} 0 & \text{if } t \le 0 \\ \dfrac{t}{t_{rr}} & \text{if } 0 < t < t_{rr} \\ 1 & \text{if } t \ge t_{rr}. \end{cases} \tag{A3}$$

This is the integral of the rectangle function

$$\mathrm{Rect}_{0,t_{rr}}(t) = \begin{cases} 0 & \text{if } t \le 0 \\ \dfrac{1}{t_{rr}} & \text{if } 0 < t < t_{rr} \\ 0 & \text{if } t \ge t_{rr}, \end{cases} \tag{A4}$$

which can be defined in terms of the unit centred rectangle,

$$\mathrm{Rect}_{0,t_{rr}}(t) = \frac{1}{t_{rr}} \mathrm{Rect}_{-1/2,1/2}\left(\frac{t - \dfrac{t_{rr}}{2}}{t_{rr}}\right). \tag{A5}$$

The Fourier transform of the latter is

$$\mathrm{Rect}_{-1/2,1/2}(f) = \frac{\sin(\pi f)}{\pi f}. \tag{A6}$$

And it is easy to derive the Fourier Transform

$$\mathrm{Rect}_{0,t_{rr}}(f) = \frac{\sin(\pi f t_{rr})}{\pi f t_{rr}} e^{-i\pi t_{rr} f}.$$

Since $\mathrm{Rect}_{0,t_{rr}}(t)$ is the derivative of $p_{\mathrm{primary}}(t)$, $i2\pi f p(f) = \mathrm{Rect}_{0,t_{rr}}(f)$,

$$p_{\mathrm{primary}}(f) = \frac{1}{i\,2\pi f} \frac{\sin(\pi f t_{rr})}{\pi f t_{rr}} e^{-i\pi t_{rr} f}. \tag{A7}$$

This statement ignores zero-frequency terms, since the integral function in the time domain is defined up to a constant. In the frequency domain, this corresponds to adding a Dirac $\delta(f)$, which only makes a difference for zero frequency. So the statement is true for the acoustic or AC case, which is the one of interest here.

Replacing the previous formula in Eq. (A2),

$$p_k = \frac{1}{i2\pi} \frac{\sin\left(\dfrac{k\pi t_{rr}}{T}\right)}{\dfrac{k\pi t_{rr}}{T}} e^{-ik\pi t_{rr}/T} (1 - e^{-ik\pi}). \tag{A8}$$

This is the formula used to plot the gray dashed line in Fig. 9.

Almeida, A., Bergeot, B., Vergez, C., and Gazengel, B. (**2015**). "Analytical determination of the attack transient in a clarinet with time-varying blowing pressure," Acta. Acust. Acust. **101**(5), 1026–1038.

Almeida, A., George, D., Smith, J., and Wolfe, J. (**2013**). "The clarinet: How blowing pressure, lip force, lip position and reed 'hardness' affect pitch, sound level, and spectrum," J. Acoust. Soc. Am. **134**, 2247–2255.

Almeida, A., Vergez, C., and Caussé, R. (**2007**). "Quasistatic nonlinear characteristics of double-reed instruments," J. Acoust. Soc. Am. **121**(1), 536–546.

Bak, N., and Dolmer, P. (**1987**). "The relation between blowing pressure and blowing frequency in clarinet playing," Acta. Acust. Acust. **63**, 238–241.

Bergeot, B., Almeida, A., Gazengel, B., Vergez, C., and Ferrand, D. (**2014**). "Response of an artificially blown clarinet to different blowing pressure profiles," J. Acoust. Soc. Am. **135**, 479–490.

Brymer, J. (**1977**). *Clarinet* (Macmillan, New York), p. 177.

Chaigne, A., and Kergomard, J. (**2016**). *Acoustics of Musical Instruments*. (Acoustical Society of America Press, Springer, New York), p. 178.

Chaudhry, M. H. (**1979**). *Applied Hydraulic Transients* (Van Nostrand Reinhold, New York), pp. 8–11.

Dalmont, J. P., Gilbert, J., Kergomard, J., and Ollivier, S. (**2005**). "An analytical prediction of the oscillation and extinction thresholds of a clarinet," J. Acoust. Soc. Am. **118**, 3294–3305.

Dalmont, J. P., Gilbert, J., and Ollivier, S. (**2003**). "Nonlinear characteristics of single-reed instruments: Quasistatic volume flow and reed opening measurements," J. Acoust. Soc. Am. **114**, 2253–2262.

Gingras, M. (**2004**). *Clarinet Secrets: 52 Performance Strategies for the Advanced Clarinetist* (Scarecrow, Lanham, MD), p. 18.

Hirschberg, A. (**1995**). "Aeroacoustics of wind instruments," in *Mechanics of Musical Instruments* (Springer, New York), Chap. 7, pp. 229–290.

Kergomard, J., Ollivier, S., and Gilbert, J. (**2000**). "Calculation of the spectrum of self-sustained oscillators using a variable truncation method," Acta. Acust. Acust. **86**, 665–703.

Li, W., Almeida, A., Smith, J., and Wolfe, J. (**2016a**). "How clarinettists articulate: The effect of blowing pressure and tonguing on initial and final transients," J. Acoust. Soc. Am. **139**, 825–838.

Li, W., Almeida, A., Smith, J., and Wolfe, J. (**2016b**). "The effect of blowing pressure, lip force and tonguing on transients: A study on clarinet-playing machine," J. Acoust. Soc. Am. **140**, 1089–1100.

Saldana, E. L., and Corso, J. F. (**1964**). "Timbre cues and the identification of musical instruments," J. Acoust. Soc. Am. **36**, 2021–2026.

Schumacher, R. T. (**1981**). "Ab initio calculations of the oscillations of a clarinet," Acustica **48**, 71–85.

Silva, F., Kergomard, J., Vergez, C., and Gilbert, J. (**2008**). "Interaction of reed and acoustic resonator in clarinetlike systems," J. Acoust. Soc. Am **124**(5), 3284–3295.

Sullivan, J. M. (**2006**). "The effects of syllabic articulation instruction on woodwind articulation accuracy," Contrib. Music Educ. **33**(1), 59–70.

Thurston, F. J. (**1977**). *Clarinet Technique* (Oxford University Press, London), p. 4.